

LARGE DISPLACEMENT ANALYSIS OF THREE-DIMENSIONAL BEAM STRUCTURES

KLAUS-JÜRGEN BATHE† AND SAÏD BOLOURCHI‡

Department of Mechanical Engineering, Massachusetts Institute of Technology, Massachusetts, U.S.A.

SUMMARY

An updated Lagrangian and a total Lagrangian formulation of a three-dimensional beam element are presented for large displacement and large rotation analysis. It is shown that the two formulations yield identical element stiffness matrices and nodal point force vectors, and that the updated Lagrangian formulation is computationally more effective. This formulation has been implemented and the results of some sample analyses are given.

INTRODUCTION

The possibility of practical static and dynamic nonlinear analysis of structures has during recent years progressed substantially, due to the effective use of digital computers operating on finite element representations of the structures. To enable general nonlinear analysis the development of versatile geometric and material nonlinear finite elements is in much need, and among these elements the use of an effective three-dimensional beam element is very important.

Since the first applications of computers to nonlinear analysis of structures, various nonlinear beam elements have been presented.¹⁻¹¹ The large number of publications on nonlinear analysis of beam structures is, at least partially, due to the fact that various kinematic nonlinear formulations can be employed, and that at this time it is not clear which formulation is most effective. The difficulty of obtaining effective solutions is particularly pronounced in the analysis of three-dimensional beam structures. Namely, considering a beam element it is noted that a general three-dimensional nonlinear beam formulation is not a simple extension of a two-dimensional formulation, because in three-dimensional analysis large rotations have to be accounted for that are not vector quantities.

In the development of a geometrically nonlinear beam element, basically an updated Lagrangian or a total Lagrangian formulation can be employed.^{12,13} These formulations must be implemented using appropriate displacement interpolation functions. Considering the choice of these functions it is recognized that for a beam of constant cross-section in small displacement analysis the Hermitian functions should be employed to interpolate the transverse bending displacements, and linear interpolation must be used to interpolate the torsional and longitudinal displacements. Therefore, in the search for a beam element that can undergo large rotations (with small strains), it is natural to employ the same functions but referred to the beam convected co-ordinate axes. In this way the usual beam kinematic assumptions are used referred to the current beam geometry.

† Associate Professor of Mechanical Engineering.

‡ Research Assistant.

Considering the formulation of a large displacement beam element, once specific beam assumptions have been made and the interpolation functions have been selected, basically the same element stiffness matrices and nodal point force vectors should be calculated using any one formulation. Therefore, the response predicted using different formulations must be the same, if the same number of beam elements are employed to model a structure. Indeed, the choice for a total Lagrangian or an updated Lagrangian formulation should be decided only by the relative numerical effectiveness of the formulations. However, considering large displacement beam formulations using the Hermitian interpolations to describe bending deformations and linear interpolations to specify axial and torsional displacements, a moving co-ordinate formulation appears quite natural. Namely, in a total Lagrangian formulation for large rotation analysis, the fact that the different displacement components are interpolated using different order polynomials establishes an interpolation directionality that requires special attention.

In another approach to formulate a beam element that includes large rotation effects, the transverse displacements, axial displacements and the rotations are interpolated independently. If the same interpolation functions are employed for all these kinematic variables, the problem of interpolation directionality under large rotations does not arise in the total Lagrangian formulation.¹⁴ However, to obtain the same accuracy as with the beam elements based on Hermitian functions, in this element formulation about twice as many degrees of freedom are needed. It can be concluded that, for straight beams, it is more efficient to employ the conventional beam interpolation functions, but to formulate more general and curved beam elements the independent interpolation of displacements and rotations is effective.

The objective in this paper is to present two consistent large rotation nonlinear three-dimensional beam formulations: an updated Lagrangian (U.L.) and a total Lagrangian (T.L.) formulation. The formulations are derived from the continuum mechanics based Lagrangian incremental equilibrium equations.¹² The beam elements are assumed to be straight, and the conventional beam displacement functions are employed to express the displacements of the elements in convected co-ordinates. In the paper the two formulations are evaluated, and it is shown that the governing incremental equilibrium equations of the beam elements are identical but that the updated Lagrangian-based element is computationally more effective. This element is a very efficient three-dimensional nonlinear beam element. The element has been implemented for use in elastic, elastic-plastic, static and dynamic analysis and in the paper a few demonstrative sample solutions are presented.

INCREMENTAL T.L. AND U.L. CONTINUUM MECHANICS FORMULATIONS

The beam element formulations are based on the general incremental T.L. and U.L. continuum mechanics equations,¹² which are briefly summarized below.

Consider the motion of a body in a fixed Cartesian co-ordinate system, as shown in Figure 1. Assume that the solutions measured in the co-ordinate system corresponding to all time points $0, \Delta t, 2\Delta t, \dots, t$ are known. It is required to solve for the unknown static and kinematic variables in the configuration at time $t + \Delta t$. In static analysis and implicit time integration the equilibrium of the body at time $t + \Delta t$ is expressed and used to solve for the static and kinematic variables corresponding to time $t + \Delta t$. On the other hand, in explicit time integration, the equilibrium at time t is employed to solve for the displacements at time $t + \Delta t$.^{12,15}

Total Lagrangian (T.L.) formulation

In the total Lagrangian formulation all static and kinematic variables are referred to the initial configuration at time 0. Considering the equilibrium of the body at time $t + \Delta t$, the principle of

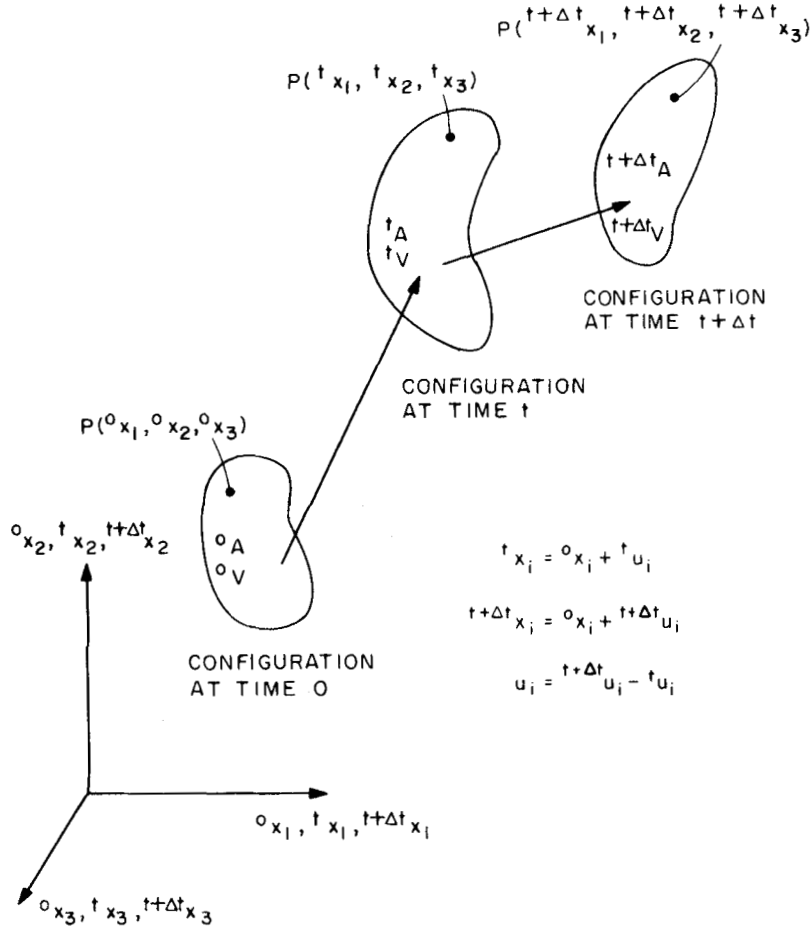


Figure 1. Motion of body in Cartesian co-ordinate system

virtual displacements gives

$$\int_{0_V} {}^{t+\Delta t} S_{ij} \delta {}^{t+\Delta t} \varepsilon_{ij} {}^0 dv = {}^{t+\Delta t} \mathcal{R} \tag{1}$$

where ${}^{t+\Delta t} \mathcal{R}$ is the total external virtual work expression due to the surface tractions with components ${}^{t+\Delta t} t_k$, and body forces with components ${}^{t+\Delta t} f_k$,

$${}^{t+\Delta t} \mathcal{R} = \int_{0_A} {}^{t+\Delta t} t_k \delta u_k {}^0 da + \int_{0_V} {}^0 \rho {}^{t+\Delta t} f_k \delta u_k {}^0 dv \tag{2}$$

In equations (1) and (2), δu_k is a (virtual) variation in the current displacement components ${}^{t+\Delta t} u_k$, $\delta {}^{t+\Delta t} \varepsilon_{ij}$ is a (virtual) variation in the Cartesian components of the Green-Lagrange strain tensor in the configuration at time $t + \Delta t$ referred to the initial configuration, and ${}^{t+\Delta t} S_{ij}$ are the Cartesian components of the 2nd Piola-Kirchhoff stress tensor in the configuration $t + \Delta t$ and

measured in the configuration at time 0:

$${}^{t+\Delta t}{}_0\epsilon_{ij} = \frac{1}{2}({}^{t+\Delta t}{}_0u_{i,j} + {}^{t+\Delta t}{}_0u_{j,i} + {}^{t+\Delta t}{}_0u_{k,i} {}^{t+\Delta t}{}_0u_{k,j}) \tag{3}$$

$${}^{t+\Delta t}{}_0S_{ij} = \frac{{}_0\rho}{{}^{t+\Delta t}\rho} {}^{t+\Delta t}{}_0x_{i,k} {}^{t+\Delta t}\tau_{kt} {}^{t+\Delta t}{}_0x_{j,l} \tag{4}$$

where ${}^{t+\Delta t}{}_0x_{i,j} = \partial^0 x_i / \partial {}^{t+\Delta t} x_j$ and the ${}^{t+\Delta t}\tau_{kt}$ are the components of the Cauchy stress tensor at time $t + \Delta t$.

In dynamic analysis the body force components in equation (2) include the mass inertia effects.¹²

Since the stresses ${}^{t+\Delta t}{}_0S_{ij}$ and strains ${}^{t+\Delta t}{}_0\epsilon_{ij}$ are unknown, for solution the following incremental decompositions are used:

$${}^{t+\Delta t}{}_0S_{ij} = {}^t{}_0S_{ij} + {}_0S_{ij} \tag{5}$$

$${}^{t+\Delta t}{}_0\epsilon_{ij} = {}^t{}_0\epsilon_{ij} + {}_0\epsilon_{ij} \tag{6}$$

where ${}^t{}_0S_{ij}$ and ${}^t{}_0\epsilon_{ij}$ are the known 2nd Piola–Kirchhoff stresses and Green–Lagrange strains in the configuration at time t . It follows from equation (6) that $\delta {}^{t+\Delta t}{}_0\epsilon_{ij} = \delta_0\epsilon_{ij}$. The strain increment components can be separated into linear and nonlinear parts

$${}_0\epsilon_{ij} = {}_0e_{ij} + {}_0\eta_{ij} \tag{7}$$

where

$${}_0e_{ij} = \frac{1}{2}[({}_0u_{i,j} + {}_0u_{j,i}) + ({}^t{}_0u_{k,i} {}_0u_{k,j} + {}^t{}_0u_{k,j} {}_0u_{k,i})] \tag{8}$$

and

$${}_0\eta_{ij} = \frac{1}{2}({}_0u_{k,i} {}_0u_{k,j}) \tag{9}$$

Finally, the constitutive relations with tensor components ${}_0C_{ijrs}$ can be used to relate incremental 2nd Piola–Kirchhoff stresses to incremental Green–Lagrange strains

$${}_0S_{ij} = {}_0C_{ijrs} {}_0\epsilon_{rs} \tag{10}$$

Using equations (5)–(10), equation (1) can now be transformed to

$$\int_{{}_0V} {}_0C_{ijrs} {}_0\epsilon_{rs} \delta_0\epsilon_{ij} {}^0dv + \int_{{}_0V} {}^t{}_0S_{ij} \delta_0\eta_{ij} {}^0dv = {}^{t+\Delta t}\mathcal{R} - \int_{{}_0V} {}^t{}_0S_{ij} \delta_0e_{ij} {}^0dv \tag{11}$$

Equation (11) is nonlinear in the incremental displacements u_i , and can be linearized by using the approximations ${}_0S_{ij} = {}_0C_{ijrs} {}_0e_{rs}$ and $\delta_0\epsilon_{ij} = \delta_0e_{ij}$. We thus obtain

$$\int_{{}_0V} {}_0C_{ijrs} {}_0e_{rs} \delta_0e_{ij} {}^0dv + \int_{{}_0V} {}^t{}_0S_{ij} \delta_0\eta_{ij} {}^0dv = {}^{t+\Delta t}\mathcal{R} - \int_{{}_0V} {}^t{}_0S_{ij} \delta_0e_{ij} {}^0dv \tag{12}$$

which is a linear equation in the incremental displacements.

Equation (12) is employed in static analysis or implicit time integration. In explicit time integration, equation (1) is used corresponding to time t .

Updated Lagrangian (U.L.) formulation

In the U.L. formulation the same incremental stress and strain decompositions as in the T.L. formulation are employed, but all variables are referred to the configuration at time t , i.e. the last known configuration. Thus, corresponding to equation (12), the linearized equilibrium equation

is in the U.L. formulation

$$\int_{V} {}^t C_{ijrs} {}^t e_{rs} \delta {}^t e_{ij} {}^t dv + \int_{V} {}^t \tau_{ij} \delta {}^t \eta_{ij} {}^t dv = {}^{t+\Delta t} \mathcal{R} - \int_{V} {}^t \tau_{ij} \delta {}^t e_{ij} {}^t dv \tag{13}$$

where the ${}^t \tau_{ij}$ are the Cartesian components of the Cauchy stress tensor at time t ; ${}^t e_{ij}$ and ${}^t \eta_{ij}$ are the Cartesian components of the linear and nonlinear strain increments, respectively, and the ${}^t C_{ijrs}$ are the components of the tangent constitutive tensor relating small strain increments to the corresponding stress increments.

U.L. AND T.L. FORMULATIONS OF BEAM ELEMENT

The general three-dimensional straight beam element is formulated based on the continuum mechanics theory summarized above. The element has two nodes with 6 degrees-of-freedom per node, and can transmit an axial force, two shear forces, two bending moments and a torque. Figure 2 shows a typical beam element.

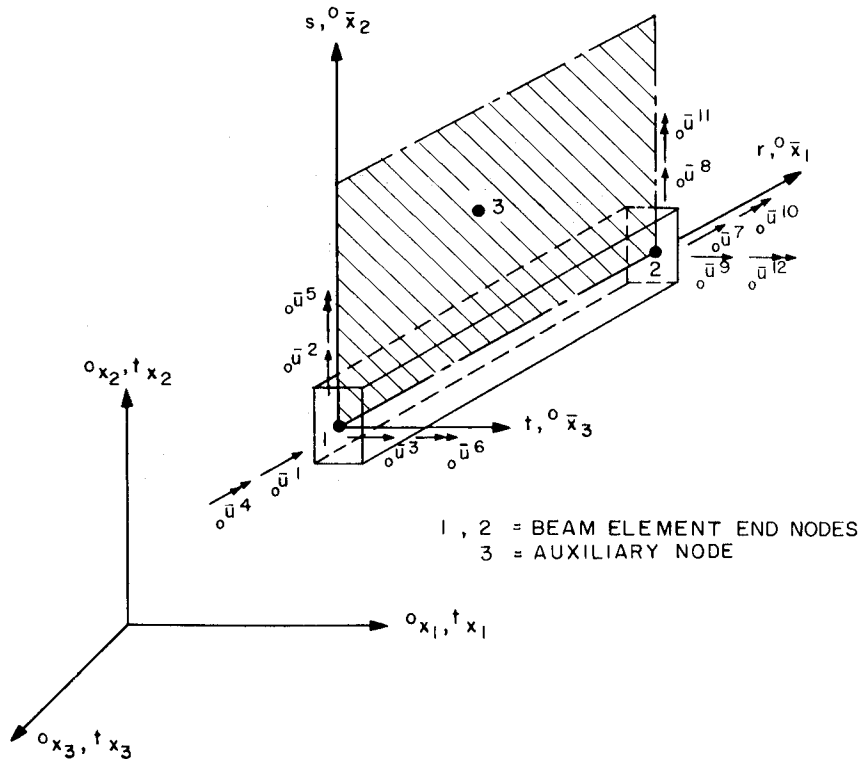


Figure 2. Schematic view of the three-dimensional beam element local co-ordinate axes

The element is assumed to be straight and of constant cross-section. It is assumed that plane sections of the beam element remain plane during deformation, but not necessarily perpendicular to the neutral axis, i.e. a constant shear is allowed. The element can undergo large deflections and rotations, but small strains are assumed. Thus, the cross-sectional area and the length of the beam element do not change during deformation.

The principal moment of inertia axes of the beam element define the local co-ordinate system r, s, t , as shown in Figure 2. The two end nodes of the element, 1 and 2, plus a third auxiliary

node, 3, are used to define these axes, where it should be noted that in the computations the r - s plane is defined by nodes 1, 2 and 3.

Incremental equilibrium equations

In equations (12) and (13) the incremental equilibrium equations of a body in motion are given corresponding to the global co-ordinate system ${}^r x_i$, $\tau = 0$ or t . Considering a typical beam element it is more effective to first evaluate the finite element matrices corresponding to the local principal axes ${}^t \bar{x}_i$ of the element (see Figure 3), and then transform the resulting matrices to correspond to the global Cartesian co-ordinate axes prior to the element assemblage process.¹⁶

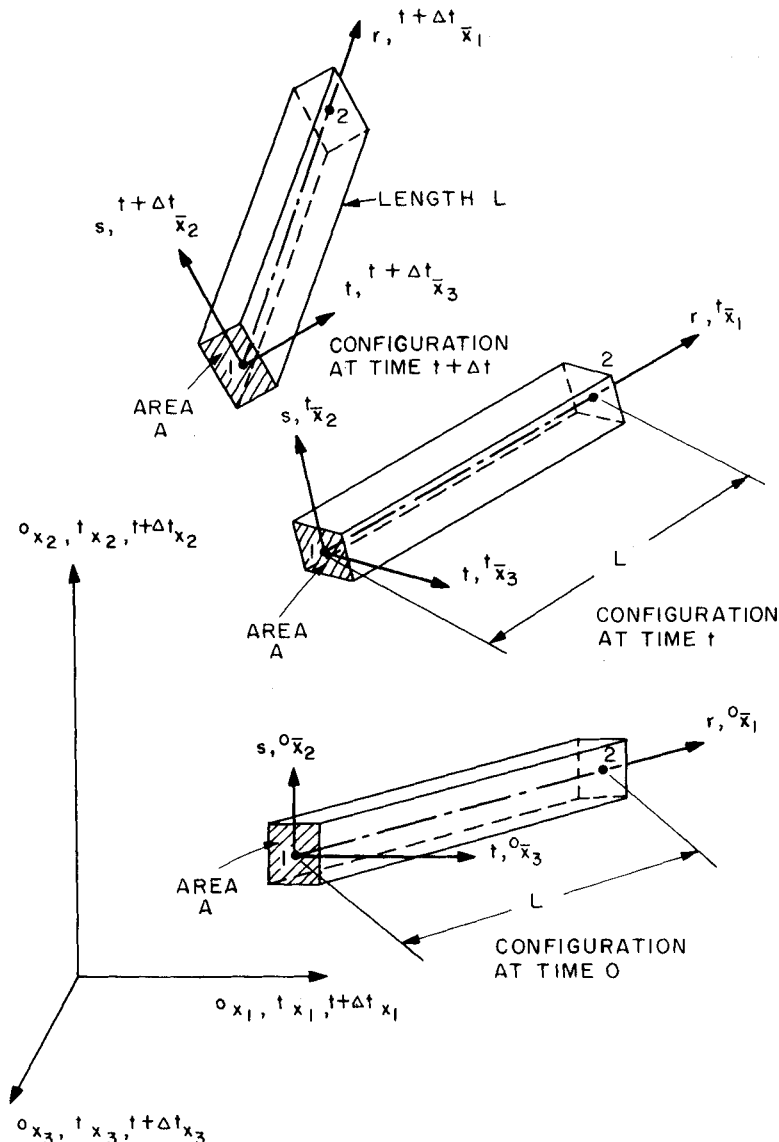


Figure 3. Motion of the three-dimensional beam element and its local co-ordinate axes shown in global co-ordinate system.

The finite element matrices corresponding to the axes ${}^{\tau}\bar{x}_i$ are simply obtained by measuring all static and kinematic quantities in this co-ordinate system. These new quantities are denoted by a bar placed over them. Thus, using equations (12) and (13) we obtain for a single beam element, using the U.L. formulation and considering only static analysis

$$({}^t\bar{\mathbf{K}}_L + {}^t\bar{\mathbf{K}}_{NL})\bar{\mathbf{u}} = {}^{t+\Delta t}\bar{\mathbf{R}} - {}^t\bar{\mathbf{F}} \tag{14}$$

and using the T.L. formulation and considering only static analysis

$$({}^t_0\mathbf{K}_L + {}^t_0\mathbf{K}_{NL})\mathbf{u} = {}^{t+\Delta t}\mathbf{R} - {}^t_0\mathbf{F} \tag{15}$$

where ${}^t_0\mathbf{K}_L, {}^t\mathbf{K}_L$ are linear strain incremental stiffness matrices; ${}^t_0\mathbf{K}_{NL}, {}^t\mathbf{K}_{NL}$ are nonlinear strain (geometric or initial stress) incremental stiffness matrices; ${}^{t+\Delta t}\mathbf{R}$ is the vector of externally applied element nodal loads at time $t + \Delta t$; ${}^t_0\mathbf{F}, {}^t\mathbf{F}$ are vectors of nodal point forces equivalent to the element stresses at time t ; and \mathbf{u} is the vector of incremental nodal displacements.

In dynamic analysis using implicit time integration the inertia forces corresponding to time $t + \Delta t$ are added to the left-hand sides of equations (14) and (15), whereas in dynamic analysis using explicit time integration the stiffness effect is not included, the inertia forces corresponding to time t are added to the left-hand sides of equations (14) and (15), and the applied external loads correspond to time t .

The element matrices in equations (14) and (15) are evaluated using the displacement interpolation functions of the beam element. Table I summarizes these calculations. The following notation is used in Table I with all quantities referred to the co-ordinate systems ${}^{\tau}\bar{x}_i, \tau = 0$ or t :

- ${}^t_0\bar{\mathbf{B}}_L, {}^t\bar{\mathbf{B}}_L$ = linear strain–displacement transformation matrices
- ${}^t_0\bar{\mathbf{B}}_{NL}, {}^t\bar{\mathbf{B}}_{NL}$ = nonlinear strain–displacement transformation matrices
- ${}^t_0\bar{\mathbf{C}}, {}^t\bar{\mathbf{C}}$ = incremental stress–strain material property matrices
- ${}^t\bar{\boldsymbol{\tau}}, {}^t\bar{\boldsymbol{\tau}}$ = matrix and vector of Cauchy stresses
- ${}^t_0\bar{\mathbf{S}}, {}^t\bar{\mathbf{S}}$ = matrix and vector of 2nd Piola–Kirchhoff stresses.

Table I. Finite element matrices

Total Lagrangian formulation	$\int_V {}^t_0\bar{C}_{ijrs} {}^t_0\bar{e}_{rs} \delta_0\bar{e}_{ij} dv$	${}^t_0\bar{\mathbf{K}}_L \bar{\mathbf{u}} = \left(\int_V {}^t_0\bar{\mathbf{B}}_L^T {}^t_0\bar{\mathbf{C}} {}^t_0\bar{\mathbf{B}}_L dv \right) \bar{\mathbf{u}}$
	$\int_V {}^t_0\bar{\mathbf{S}}_{ij} \delta_0\bar{\eta}_{ij} dv$	${}^t_0\bar{\mathbf{K}}_{NL} \bar{\mathbf{u}} = \left(\int_V {}^t_0\bar{\mathbf{B}}_{NL}^T {}^t_0\bar{\mathbf{S}} {}^t_0\bar{\mathbf{B}}_{NL} dv \right) \bar{\mathbf{u}}$
	$\int_V {}^t_0\bar{\mathbf{S}}_{ij} \delta_0\bar{e}_{ij} dv$	${}^t_0\bar{\mathbf{F}} = \int_V {}^t_0\bar{\mathbf{B}}_L^T {}^t_0\bar{\mathbf{S}} dv$
Updated Lagrangian formulation	$\int_V {}^t\bar{C}_{ijrs} {}^t\bar{e}_{rs} \delta_t\bar{e}_{ij} dv$	${}^t\bar{\mathbf{K}}_L \bar{\mathbf{u}} = \left(\int_V {}^t\bar{\mathbf{B}}_L^T {}^t\bar{\mathbf{C}} {}^t\bar{\mathbf{B}}_L dv \right) \bar{\mathbf{u}}$
	$\int_V {}^t\bar{\mathbf{S}}_{ij} \delta_t\bar{\eta}_{ij} dv$	${}^t\bar{\mathbf{K}}_{NL} \bar{\mathbf{u}} = \left(\int_V {}^t\bar{\mathbf{B}}_{NL}^T {}^t\bar{\mathbf{S}} {}^t\bar{\mathbf{B}}_{NL} dv \right) \bar{\mathbf{u}}$
	$\int_V {}^t\bar{\mathbf{S}}_{ij} \delta_t\bar{e}_{ij} dv$	${}^t\bar{\mathbf{F}} = \int_V {}^t\bar{\mathbf{B}}_L^T {}^t\bar{\mathbf{S}} dv$

It should be noted that the elements of the stress matrices and vectors in the T.L. and the U.L. formulations are equal, because small strain conditions are assumed.

Interpolation functions for incremental displacements

To describe the motion of the beam elements the incremental displacement field within the elements as a function of the incremental nodal point displacement components is required,

$${}^t\bar{u}_i = \sum_{k=1}^N {}^t h_k^i {}^t\bar{u}^k \quad (16)$$

where the ${}^t h_k^i$ are the interpolation functions corresponding to the local axes ${}^t\bar{x}_i$, and the ${}^t\bar{u}^k$ are the nodal point displacement increments measured in the local axes at time t (see Figure 3).

The interpolation functions in equation (16) are constructed assuming cubic bending displacement variations and a linear variation in the axial and torsional displacements. In order to include shear effects, constant shear deformations can be included. Using the usual beam incremental nodal displacements (these are shown for time 0 in Figure 2) and leaving the shear deformations as independent variables, we obtain the incremental displacement interpolation functions given in Table II. In this table the variable N in equation (16) is equal to 12 if no shear deformations are included; otherwise N is equal to 14. If shear deformations are included the element stiffness matrices and nodal point force vectors are of order 14, and are reduced to order 12 by static condensation prior to the element assemblage process.

Strain-displacement transformation matrices in the U.L. formulation

The kinematic assumptions used in defining the interpolation functions of Table II hold for small strains, small rigid body incremental rotations in each solution step, but any size translational displacements. These assumptions are appropriate for the updated Lagrangian formulation of beams, because the kinematic variables are linearized about the last-known body position.

Using the interpolation functions in Table II, the strain-displacement matrices of the U.L. formulation can directly be evaluated. Table III(B) summarizes the calculation of the matrices ${}^t\bar{\mathbf{B}}_L$ and ${}^t\bar{\mathbf{B}}_{NL}$ that are required to evaluate the tangent stiffness matrix and nodal point force vector of an element corresponding to co-ordinate axes ${}^t\bar{x}_i$ ($i = 1, 2, 3$). The element matrices have to be transformed to the global co-ordinate system prior to their assemblage into a system of beam elements.

Strain-displacement transformation matrices in the T.L. formulation

In the discussion of the total Lagrangian formulation and the comparative study of the total and updated Lagrangian formulations we do not include, for clarity, the effect of shear deformations. Referring to the definitions in Figures 2 and 3, the displacement increments within the element at time t measured in the local axes at time 0 are related to the nodal point displacement increments of the element in its local axes using

$${}^0\bar{u}_i = \sum_{k=1}^{12} {}^0 h_k^i {}^0\bar{u}^k \quad (17)$$

where the ${}^0\bar{u}^k$ are the element nodal point displacement increments at time t , but measured in the ${}^0\bar{x}_i$ ($i = 1, 2, 3$) co-ordinate system. The functions ${}^0 h_k^i$ ($i = 1, 2, 3$) are the interpolation

Table II. Beam interpolation functions

We define:

$$\begin{aligned} \psi_1 &= \frac{r}{L} - \left(\frac{r}{L}\right)^2; & \psi_2 &= 1 - 4\frac{r}{L} + 3\left(\frac{r}{L}\right)^2; & \psi_3 &= 2\frac{r}{L} - 3\left(\frac{r}{L}\right)^2 \\ \psi_4 &= 1 - 3\left(\frac{r}{L}\right)^2 + 2\left(\frac{r}{L}\right)^3; & \psi_5 &= \frac{r}{L} - 2\left(\frac{r}{L}\right)^2 + \left(\frac{r}{L}\right)^3 \\ \psi_6 &= 3\left(\frac{r}{L}\right)^2 - 2\left(\frac{r}{L}\right)^3; & \psi_7 &= \frac{r}{L} - 3\left(\frac{r}{L}\right)^2 + 2\left(\frac{r}{L}\right)^3 \end{aligned}$$

Incremental displacement interpolation matrix

$${}^i\bar{\mathbf{H}} = \begin{bmatrix} {}^i\mathbf{h}^1 \\ {}^i\mathbf{h}^2 \\ {}^i\mathbf{h}^3 \end{bmatrix} = \begin{bmatrix} 1 - \frac{r}{L} & 6\psi_1 \frac{s}{L} & 6\psi_1 \frac{t}{L} & 0 & \psi_2 t & -\psi_2 s & \frac{r}{L} \\ 0 & \psi_4 & 0 & -\left(1 - \frac{r}{L}\right)t & 0 & \psi_5 L & 0 \\ 0 & 0 & \psi_4 & \left(1 - \frac{r}{L}\right)s & -\psi_5 L & 0 & 0 \\ & -6\psi_1 \frac{s}{L} & -6\psi_1 \frac{t}{L} & 0 & -\psi_3 t & \psi_3 s & -(1 - 6\psi_1)t & (1 - 6\psi_1)s \\ & \psi_6 & 0 & -\frac{r}{L}t & 0 & -\psi_1 r & 0 & (r - \psi_7 L) \\ & 0 & \psi_6 & \frac{r}{L}s & \psi_1 r & 0 & (r - \psi_7 L) & 0 \end{bmatrix}$$

where

L = length of the beam element

${}^i\mathbf{h}^i$ = vector of interpolation functions in ${}^i\bar{x}_i$ direction

r, s, t = beam convected co-ordinate axes (see Figure 3)

The incremental displacement vector is

$${}^i\bar{\mathbf{u}}^T = [{}^i\bar{u}^1 \quad {}^i\bar{u}^2 \quad \dots \quad {}^i\bar{u}^{12} \quad {}^i\bar{u}^{13} \quad {}^i\bar{u}^{14}]$$

where ${}^i\bar{u}^{13} \equiv \beta_1$, ${}^i\bar{u}^{14} \equiv \beta_2$ (shear deformations)

functions corresponding to the convected axes r, s, t and measured in the co-ordinate system ${}^0\bar{x}_j$ ($j = 1, 2, 3$).

The interpolation functions ${}^0h_k^i$ are obtained using

$${}^0h_k^i = \sum_{m=1}^3 \sum_{n=1}^{12} {}^i\bar{\mathbf{R}}_{im} {}^m h_n^m {}^i\bar{\mathbf{R}}_{nk} \tag{18}$$

Table III. Matrices used in beam analysis

A. TOTAL LAGRANGIAN FORMULATION

1. Incremental strains

$${}^0\bar{\epsilon}_{ij} = {}^0\bar{\epsilon}_{ij} + {}^0\bar{\eta}_{ij}$$

$${}^0\bar{\epsilon}_{11} = {}^0\bar{u}_{1,1} + {}^0\bar{u}_{1,1} + {}^0\bar{u}_{2,1} + {}^0\bar{u}_{3,1} + \frac{1}{2}[({}^0\bar{u}_{1,1})^2 + ({}^0\bar{u}_{2,1})^2 + ({}^0\bar{u}_{3,1})^2]$$

$${}^0\bar{\epsilon}_{12} = \frac{1}{2}\{[{}^0\bar{u}_{1,2} + {}^0\bar{u}_{2,1}] + [{}^0\bar{u}_{1,1} {}^0\bar{u}_{1,2} + {}^0\bar{u}_{2,1} {}^0\bar{u}_{2,2} + {}^0\bar{u}_{3,1} {}^0\bar{u}_{3,2} + {}^0\bar{u}_{1,2} {}^0\bar{u}_{1,1} + {}^0\bar{u}_{2,2} {}^0\bar{u}_{2,1} + {}^0\bar{u}_{3,2} {}^0\bar{u}_{3,1}]\}$$

$$+ \frac{1}{2}\{[{}^0\bar{u}_{1,1} {}^0\bar{u}_{1,2} + {}^0\bar{u}_{2,1} {}^0\bar{u}_{2,2} + {}^0\bar{u}_{3,1} {}^0\bar{u}_{3,2}]\}$$

$${}^0\bar{\epsilon}_{13} = \frac{1}{2}\{[{}^0\bar{u}_{1,3} + {}^0\bar{u}_{3,1}] + [{}^0\bar{u}_{1,1} {}^0\bar{u}_{1,3} + {}^0\bar{u}_{2,1} {}^0\bar{u}_{2,3} + {}^0\bar{u}_{3,1} {}^0\bar{u}_{3,3} + {}^0\bar{u}_{1,3} {}^0\bar{u}_{1,1} + {}^0\bar{u}_{2,3} {}^0\bar{u}_{2,1} + {}^0\bar{u}_{3,3} {}^0\bar{u}_{3,1}]\}$$

$$+ \frac{1}{2}\{[{}^0\bar{u}_{1,1} {}^0\bar{u}_{1,3} + {}^0\bar{u}_{2,1} {}^0\bar{u}_{2,3} + {}^0\bar{u}_{3,1} {}^0\bar{u}_{3,3}]\}$$

where

$${}^0\bar{u}_{i,j} = \frac{\partial {}^0\bar{u}_i}{\partial {}^0\bar{x}_j}; \quad {}^0\bar{u}_{i,i} = \frac{\partial {}^0\bar{u}_i}{\partial {}^0\bar{x}_i}; \quad {}^0\bar{x}_1 \equiv r, \quad {}^0\bar{x}_2 \equiv s, \quad {}^0\bar{x}_3 \equiv t$$

2. Linear strain-displacement transformation matrix

Using

$${}^0\bar{\epsilon} = {}^0\bar{\mathbf{B}}_L {}^0\bar{\mathbf{u}}; \quad {}^0\bar{\mathbf{u}} = {}^0\mathbf{R}\mathbf{u}$$

where

${}^0\bar{\mathbf{u}}$ = vector of incremental nodal displacements measured in ${}^0\bar{x}_i$ ($i = 1, 2, 3$) co-ordinate system

\mathbf{u} = vector of incremental nodal displacements in global co-ordinate system

${}^0\mathbf{R}$ = transformation matrix

and

$${}^0\bar{\epsilon}^T = [{}^0\bar{\epsilon}_{11} \quad 2{}^0\bar{\epsilon}_{12} \quad 2{}^0\bar{\epsilon}_{13}]; \quad {}^0\bar{\mathbf{u}}^T = [{}^0\bar{u}^1 \quad {}^0\bar{u}^2 \quad {}^0\bar{u}^3 \quad \dots \quad {}^0\bar{u}^{12}]$$

$${}^0\bar{\mathbf{B}}_L = {}^0\bar{\mathbf{B}}_{L0} + {}^0\bar{\mathbf{B}}_{L1}$$

where

$${}^0\bar{\mathbf{B}}_{L0} = \begin{bmatrix} {}^0h^1_{1,1} & {}^0h^1_{2,1} & {}^0h^1_{3,1} & \dots & {}^0h^1_{12,1} \\ ({}^0h^1_{1,2} + {}^0h^2_{1,1}) & ({}^0h^1_{2,2} + {}^0h^2_{2,1}) & ({}^0h^1_{3,2} + {}^0h^2_{3,1}) & \dots & ({}^0h^1_{12,2} + {}^0h^2_{12,1}) \\ ({}^0h^1_{1,3} + {}^0h^3_{1,1}) & ({}^0h^1_{2,3} + {}^0h^3_{2,1}) & ({}^0h^1_{3,3} + {}^0h^3_{3,1}) & \dots & ({}^0h^1_{12,3} + {}^0h^3_{12,1}) \end{bmatrix}$$

and

$${}^0\bar{\mathbf{B}}_{L1} = \begin{bmatrix} (l_{11} {}^0h^1_{1,1} + l_{21} {}^0h^2_{1,1} + l_{31} {}^0h^3_{1,1}) \\ (l_{11} {}^0h^1_{1,2} + l_{12} {}^0h^1_{1,1} + l_{21} {}^0h^2_{1,2} + l_{22} {}^0h^2_{1,1} + l_{31} {}^0h^3_{1,2} + l_{32} {}^0h^3_{1,1}) \\ (l_{11} {}^0h^1_{1,3} + l_{13} {}^0h^1_{1,1} + l_{21} {}^0h^2_{1,3} + l_{23} {}^0h^2_{1,1} + l_{31} {}^0h^3_{1,3} + l_{33} {}^0h^3_{1,1}) \\ (l_{11} {}^0h^1_{2,1} + l_{21} {}^0h^2_{2,1} + l_{31} {}^0h^3_{2,1}) \dots \\ (l_{11} {}^0h^1_{2,2} + l_{12} {}^0h^1_{2,1} + l_{21} {}^0h^2_{2,2} + l_{22} {}^0h^2_{2,1} + l_{31} {}^0h^3_{2,2} + l_{32} {}^0h^3_{2,1}) \dots \\ (l_{11} {}^0h^1_{2,3} + l_{13} {}^0h^1_{2,1} + l_{21} {}^0h^2_{2,3} + l_{23} {}^0h^2_{2,1} + l_{31} {}^0h^3_{2,3} + l_{33} {}^0h^3_{2,1}) \dots \\ \dots (l_{11} {}^0h^1_{12,1} + l_{21} {}^0h^2_{12,1} + l_{31} {}^0h^3_{12,1}) \\ \dots (l_{11} {}^0h^1_{12,2} + l_{12} {}^0h^1_{12,1} + l_{21} {}^0h^2_{12,2} + l_{22} {}^0h^2_{12,1} + l_{31} {}^0h^3_{12,2} + l_{32} {}^0h^3_{12,1}) \\ \dots (l_{11} {}^0h^1_{12,3} + l_{13} {}^0h^1_{12,1} + l_{21} {}^0h^2_{12,3} + l_{23} {}^0h^2_{12,1} + l_{31} {}^0h^3_{12,3} + l_{33} {}^0h^3_{12,1}) \end{bmatrix}$$

Table III—continued

where

$$l_{ij} = \frac{\partial^1 \bar{u}_i}{\partial^0 \bar{x}_j}$$

3. Nonlinear strain–displacement transformation matrix

$${}^0\bar{\mathbf{B}}_{NL} = \begin{bmatrix} {}_0h_{1,1}^1 & {}_0h_{2,1}^1 & {}_0h_{3,1}^1 & \dots & {}_0h_{12,1}^1 \\ {}_0h_{1,1}^2 & {}_0h_{2,1}^2 & {}_0h_{3,1}^2 & \dots & {}_0h_{12,1}^2 \\ {}_0h_{1,1}^3 & {}_0h_{2,1}^3 & {}_0h_{3,1}^3 & \dots & {}_0h_{12,1}^3 \\ {}_0h_{1,2}^1 & {}_0h_{2,2}^1 & {}_0h_{3,2}^1 & \dots & {}_0h_{12,2}^1 \\ {}_0h_{1,2}^2 & {}_0h_{2,2}^2 & {}_0h_{3,2}^2 & \dots & {}_0h_{12,2}^2 \\ {}_0h_{1,2}^3 & {}_0h_{2,2}^3 & {}_0h_{3,2}^3 & \dots & {}_0h_{12,2}^3 \\ {}_0h_{1,3}^1 & {}_0h_{2,3}^1 & {}_0h_{3,3}^1 & \dots & {}_0h_{12,3}^1 \\ {}_0h_{1,3}^2 & {}_0h_{2,3}^2 & {}_0h_{3,3}^2 & \dots & {}_0h_{12,3}^2 \\ {}_0h_{1,3}^3 & {}_0h_{2,3}^3 & {}_0h_{3,3}^3 & \dots & {}_0h_{12,3}^3 \end{bmatrix}$$

4. 2nd Piola–Kirchhoff stress matrix and vector

$${}^0\bar{\mathbf{S}} = \begin{bmatrix} {}^0\bar{\mathbf{S}}_{11}\mathbf{I}_3 & \text{symmetric} \\ {}^0\bar{\mathbf{S}}_{12}\mathbf{I}_3 & \mathbf{0} \\ {}^0\bar{\mathbf{S}}_{13}\mathbf{I}_3 & \mathbf{0} \end{bmatrix}; \quad {}^0\bar{\mathbf{S}} = \begin{bmatrix} {}^0\bar{\mathbf{S}}_{11} \\ {}^0\bar{\mathbf{S}}_{12} \\ {}^0\bar{\mathbf{S}}_{13} \end{bmatrix}$$

where \mathbf{I}_3 is a 3×3 identity matrix.

B. UPDATED LAGRANGIAN FORMULATION

1. Incremental strains

$$\begin{aligned} {}_t\bar{\epsilon}_{ij} &= {}_t\bar{\epsilon}_{ij} + {}_t\bar{\eta}_{ij} \\ {}_t\bar{\epsilon}_{11} &= {}_t\bar{u}_{1,1} + \frac{1}{2}[({}_t\bar{u}_{1,1})^2 + ({}_t\bar{u}_{2,1})^2 + ({}_t\bar{u}_{3,1})^2] \\ {}_t\bar{\epsilon}_{12} &= \frac{1}{2}[_t\bar{u}_{1,2} + {}_t\bar{u}_{2,1}] + \frac{1}{2}[_t\bar{u}_{1,1} {}_t\bar{u}_{1,2} + {}_t\bar{u}_{3,1} {}_t\bar{u}_{3,2}] \\ {}_t\bar{\epsilon}_{13} &= \frac{1}{2}[_t\bar{u}_{1,3} + {}_t\bar{u}_{3,1}] + \frac{1}{2}[_t\bar{u}_{1,1} {}_t\bar{u}_{1,3} + {}_t\bar{u}_{2,1} {}_t\bar{u}_{2,3}] \end{aligned}$$

where

$${}_t\bar{u}_{i,j} = \frac{\partial_i \bar{u}_i}{\partial^j \bar{x}_j}; \quad {}^t\bar{x}_j \quad (j = 1, 2, 3) \equiv r, s, t$$

2. Linear strain–displacement transformation matrix

Using

$${}_t\bar{\mathbf{e}} = {}^t\bar{\mathbf{B}}_L {}_t\bar{\mathbf{u}}$$

where

$${}_t\bar{\mathbf{e}}^T = [{}_t\bar{\epsilon}_{11} \quad 2{}_t\bar{\epsilon}_{12} \quad 2{}_t\bar{\epsilon}_{13}]$$

and

$${}_t\bar{\mathbf{u}} = {}^t\mathbf{R} \mathbf{u}$$

Table III—continued

where

$\bar{\mathbf{u}}$ = vector of incremental nodal displacements measured in the ${}^t\bar{x}_i$ ($i = 1, 2, 3$) co-ordinate system

\mathbf{u} = vector of incremental nodal displacements in the global co-ordinate system

${}^t\mathbf{R}$ = transformation matrix between the local co-ordinate system at time t and the global co-ordinate system

$${}^t\bar{\mathbf{B}}_L = \begin{bmatrix} h_{1,1}^1 & h_{2,1}^1 & h_{3,1}^1 & \dots & h_{N,1}^1 \\ (h_{1,2}^1 + h_{1,1}^2) & (h_{2,2}^1 + h_{2,1}^2) & (h_{3,2}^1 + h_{3,1}^2) & \dots & (h_{N,2}^1 + h_{N,1}^2) \\ (h_{1,3}^1 + h_{1,1}^3) & (h_{2,3}^1 + h_{2,1}^3) & (h_{3,3}^1 + h_{3,1}^3) & \dots & (h_{N,3}^1 + h_{N,1}^3) \end{bmatrix}$$

where

$$h_{k,j}^i = \frac{\partial_i h_k^i}{\partial {}^t\bar{x}_j} \quad \begin{matrix} N = 12 \text{ if shear effects are neglected} \\ N = 14 \text{ if shear effects are included} \end{matrix}$$

3. Nonlinear strain-displacement transformation matrix

$${}^t\bar{\mathbf{B}}_{NL} = \begin{bmatrix} h_{1,1}^1 & h_{2,1}^1 & h_{3,1}^1 & \dots & h_{N,1}^1 \\ h_{1,1}^2 & h_{2,1}^2 & h_{3,1}^2 & \dots & h_{N,1}^2 \\ h_{1,1}^3 & h_{2,1}^3 & h_{3,1}^3 & \dots & h_{N,1}^3 \\ h_{1,2}^1 & h_{2,2}^1 & h_{3,2}^1 & \dots & h_{N,2}^1 \\ h_{1,2}^2 & h_{2,2}^2 & h_{3,2}^2 & \dots & h_{N,2}^2 \\ h_{1,2}^3 & h_{2,2}^3 & h_{3,2}^3 & \dots & h_{N,2}^3 \\ h_{1,3}^1 & h_{2,3}^1 & h_{3,3}^1 & \dots & h_{N,3}^1 \\ h_{1,3}^2 & h_{2,3}^2 & h_{3,3}^2 & \dots & h_{N,3}^2 \end{bmatrix}$$

4. Cauchy stress matrix and stress vector

$${}^t\bar{\boldsymbol{\tau}} = \begin{bmatrix} {}^t\bar{\tau}_{11} & & & & & & & & \\ 0 & {}^t\bar{\tau}_{11} & & & & & & & \\ 0 & 0 & {}^t\bar{\tau}_{11} & & & & & & \\ {}^t\bar{\tau}_{12} & 0 & 0 & 0 & & & & & \\ 0 & 0 & {}^t\bar{\tau}_{12} & 0 & 0 & & & & \\ {}^t\bar{\tau}_{13} & 0 & 0 & 0 & 0 & 0 & & & \\ 0 & {}^t\bar{\tau}_{13} & 0 & 0 & 0 & 0 & 0 & & \\ & & & & & & & & 0 \end{bmatrix}; \quad {}^t\bar{\boldsymbol{\tau}} = \begin{bmatrix} {}^t\bar{\tau}_{11} \\ {}^t\bar{\tau}_{12} \\ {}^t\bar{\tau}_{13} \end{bmatrix}$$

where ${}^t\bar{R}_{im}$ is the element (i, m) of the matrix ${}^t\bar{\mathbf{R}}$, which transforms displacements measured in the co-ordinate system ${}^t\bar{x}_i$ ($i = 1, 2, 3$) to displacements measured in the system ${}^0\bar{x}_i$ ($i = 1, 2, 3$) as defined in equation (22).

A typical derivative required in the calculation of the strain-displacement transformation matrix is $(\partial_0 \bar{u}_i / \partial {}^0\bar{x}_j) = \sum_{k=1}^{12} (\partial_0 h_k^i / \partial {}^0\bar{x}_j) {}^0\bar{u}^k$. To evaluate these derivatives it should be noted that the axes ${}^0\bar{x}_j$ ($j = 1, 2, 3$) correspond to the convected co-ordinates axes r, s, t at time 0 (i.e. ${}^0\bar{x}_1 \equiv r; {}^0\bar{x}_2 \equiv s; {}^0\bar{x}_3 \equiv t$). Using Eq. (18) we have

$$\frac{\partial_0 \bar{u}_i}{\partial {}^0\bar{x}_j} = \sum_{k=1}^{12} \sum_{m=1}^3 \sum_{n=1}^{12} {}^t\bar{R}_{im} \frac{\partial h_n^m}{\partial {}^0\bar{x}_j} {}^t\bar{R}_{nk} {}^0\bar{u}^k \tag{19}$$

Therefore, double transformations are needed for the strain calculations in the T.L. formulation. In comparison, the U.L. formulation does not require the above transformation.

In order to evaluate the strain increments it is also necessary to calculate the derivatives of the total displacements. The kinematics of the rigid body rotations of the beam give

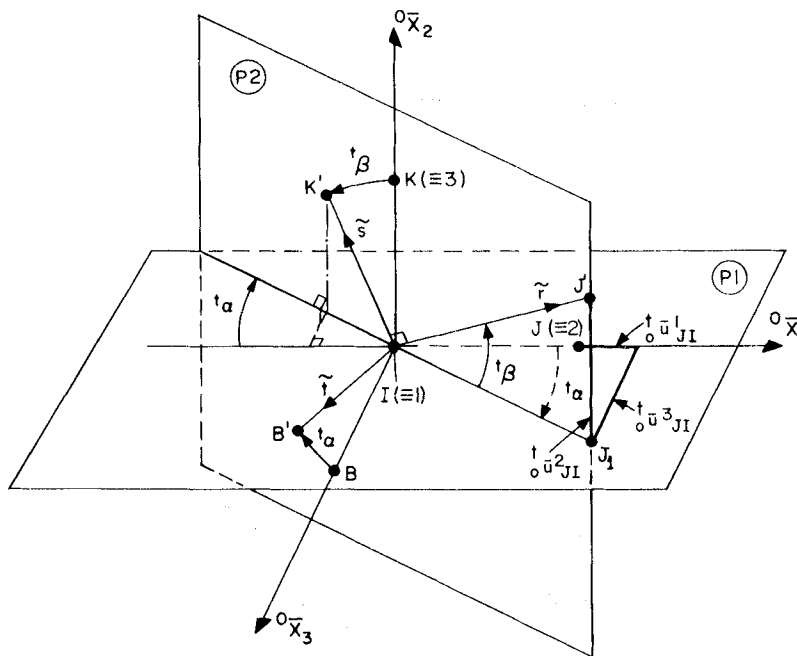
$${}^i_0\bar{u}_{i,j} = {}^i\bar{R}_{ij} - \delta_{ij} \quad \begin{matrix} (i = 1, 2, 3) \\ (j = 1, 2, 3) \end{matrix} \quad (20)$$

where the ${}^i\bar{R}_{ij}$ are the direction cosines of the ${}^i\bar{x}_i$ axes with respect to the ${}^0\bar{x}_i$ axes, as defined in equation (23), and δ_{ij} is the Kronecker delta.

Transformation between current and original beam co-ordinate axes

In the U.L. and T.L. formulations a transformation matrix ${}^i\bar{\mathbf{R}}$ that relates displacements measured in the current configuration to displacements measured in the original configuration is needed.

The ${}^i\bar{\mathbf{R}}$ transformation matrix is evaluated using Euler angles which define the rotations of the beam. These angles are shown in Figures 4(a) and 4(b). To arrive at the information given in this illustration it is required first to evaluate the relative translational displacements of nodes

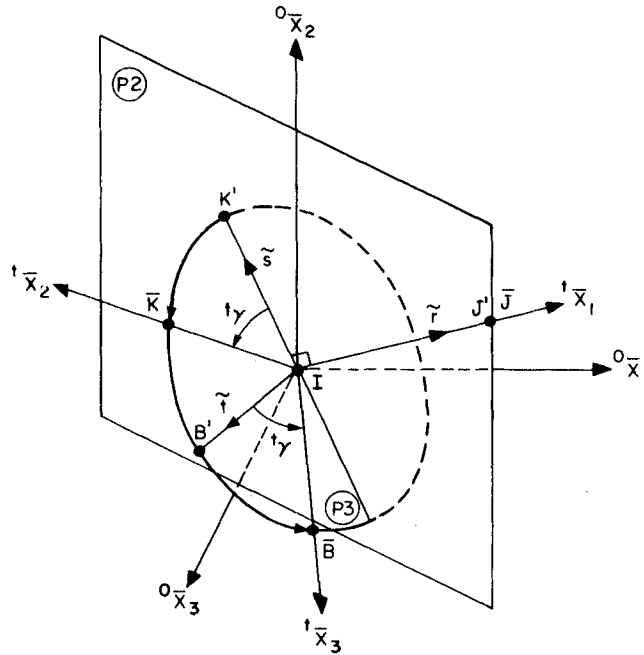


α = ROTATION OF COORDINATE AXES ABOUT ${}^0\bar{x}_2$ AXIS
 $({}^0\bar{x}_1, {}^0\bar{x}_2, {}^0\bar{x}_3)$ TO $({}^i\bar{J}_1, {}^0\bar{x}_2, \tilde{\tau})$

β = ROTATION OF COORDINATE AXES ABOUT $\tilde{\tau}$ AXIS
 $({}^i\bar{J}_1, {}^0\bar{x}_2, \tilde{\tau})$ TO $(\tilde{\tau}, \tilde{s}, \tilde{\tau})$

PLANE P1 IS PERPENDICULAR TO PLANE P2

Figure 4(a). Rotation of beam element co-ordinate axes in large displacement analysis (first step).



γ = ROTATION OF COORDINATE AXES ABOUT \tilde{z} AXIS
 ($\tilde{x}, \tilde{s}, \tilde{z}$) TO (${}^1\bar{x}_1, {}^1\bar{x}_2, {}^1\bar{x}_3$)

PLANE P3 IS PERPENDICULAR TO \tilde{z} AXIS

Figure 4(b). Rotation of beam element co-ordinate axes in large displacement analysis (final step).

1 and 2 measured in the beam original co-ordinate system. Denoting for clarity nodes 1 and 2 as nodes I and J , these relative displacements are evaluated as

$${}^i_0\bar{u}_{II} = {}^0R_{ij}({}^t u^{j+6} - {}^t u^j) \quad \left(\begin{array}{l} i = 1, 2, 3 \\ \text{sum on } j = 1, 2, 3 \end{array} \right) \quad (21)$$

where the ${}^t u^k$ are the element nodal point displacements measured in the global co-ordinate system, and the ${}^0R_{ij}$ are components of the matrix ${}^0\mathbf{R}$ that transforms the global nodal point displacements to the element local axes at time 0.

The components of the matrix ${}^t\bar{\mathbf{R}}$ are then constructed from the direction cosines of the axes ${}^t\bar{x}_i$ ($i = 1, 2, 3$) with respect to the axes ${}^0\bar{x}_j$ ($j = 1, 2, 3$). We have

$${}^t\bar{\mathbf{R}} = \begin{bmatrix} {}^t\bar{\mathbf{R}} & & 0 \\ & {}^t\bar{\mathbf{R}} & \\ 0 & & {}^t\bar{\mathbf{R}} \end{bmatrix} \quad (22)$$

where ${}^t\bar{\mathbf{R}}$ is a matrix of order 3×3 ,

$${}^t\bar{\mathbf{R}} = {}^t\bar{\mathbf{R}}^a {}^t\bar{\mathbf{R}}^d \quad (23)$$

In equation (23) ${}^t\bar{\mathbf{R}}^d$ is the transformation matrix due to the relative translational displacements of nodes J and I , and ${}^t\bar{\mathbf{R}}^a$ is the transformation matrix that takes into account the axial rotation of the beam.

The components of the matrix ${}^t\bar{\mathbf{R}}^d$ are the direction cosines of the axes $\tilde{r}, \tilde{s}, \tilde{t}$ with respect to ${}^0\tilde{x}_i$ ($i = 1, 2, 3$). These components are

$${}^t\bar{\mathbf{R}}^d = \begin{bmatrix} \cos({}^t\alpha) \cos({}^t\beta) & \sin({}^t\beta) & \sin({}^t\alpha) \cos({}^t\beta) \\ -\cos({}^t\alpha) \sin({}^t\beta) & \cos({}^t\beta) & -\sin({}^t\alpha) \sin({}^t\beta) \\ -\sin({}^t\alpha) & 0 & \cos({}^t\alpha) \end{bmatrix} \quad (24)$$

where the angle ${}^t\alpha$ represents the rotation about the (negative) ${}^0\tilde{x}_2$ axis

$$\cos({}^t\alpha) = \frac{{}^0L + {}^t\bar{u}_{JI}^1}{\bar{I}J_1} \quad (25)$$

and 0L is the original length of the beam,

$$\bar{I}J_1 = \{({}^0L + {}^t\bar{u}_{JI}^1)^2 + ({}^t\bar{u}_{JI}^3)^2\}^{1/2} \quad (26)$$

The angle ${}^t\beta$ represents the rotation about the positive \tilde{t} direction;

$$\sin({}^t\beta) = \frac{{}^t\bar{u}_{JI}^2}{{}^tL} \quad (27)$$

where

$${}^tL = \{(\bar{I}J_1)^2 + ({}^t\bar{u}_{JI}^2)^2\}^{1/2} \quad (28)$$

The components of the ${}^t\bar{\mathbf{R}}^a$ matrix, which are the direction cosines between ${}^t\tilde{x}_i$ ($i = 1, 2, 3$) and the $\tilde{r}, \tilde{s}, \tilde{t}$ axes are computed using

$${}^t\bar{\mathbf{R}}^a = \begin{bmatrix} 1 & 0 & 0 \\ 0 & \cos({}^t\gamma) & \sin({}^t\gamma) \\ 0 & -\sin({}^t\gamma) & \cos({}^t\gamma) \end{bmatrix} \quad (29)$$

where ${}^t\gamma$ is the rigid body rotation of the beam about the \tilde{r} -axis in the configuration at time t . This angle is calculated using

$$\begin{aligned} \gamma &= \frac{1}{2}\{{}^t\bar{u}^4 + {}^t\bar{u}^{10}\} \\ &= \frac{1}{2}\{{}^t\bar{\mathbf{R}}_{11}^d ({}^0\bar{u}^4 + {}^0\bar{u}^{10}) + {}^t\bar{\mathbf{R}}_{12}^d ({}^0\bar{u}^5 + {}^0\bar{u}^{11}) + {}^t\bar{\mathbf{R}}_{13}^d ({}^0\bar{u}^6 + {}^0\bar{u}^{12})\} \end{aligned} \quad (30)$$

and then

$${}^t\gamma = {}^{t-\Delta t}\gamma + \gamma \quad (31)$$

Substituting the relations in equations (23)–(31) into equation (22) we obtain the transformation matrix between the beam local axes at times t and 0.

Calculation of beam element stresses

In the development of the incremental U.L. and T.L. equilibrium equations corresponding to time t , we assumed that the stress components corresponding to the configuration at time t are known (see Table I). The solution of the incremental equations (14) and (15) will then yield nodal point displacement increments, from which the corresponding stress increments must be calculated. These stress increments are added to the stress components at time t to obtain the stress components corresponding to time $t + \Delta t$.

To evaluate the stress increments accurately it is realized that the tangent approximation in the strain–displacement relation for the normal strain, as employed in the ${}^t\bar{\mathbf{B}}_L$ and ${}^0\bar{\mathbf{B}}_L$ matrices, does not yield an increment in normal strain if the element deflects transversely without bending. However, for large displacement analysis, the corresponding extension of the element is taken into account in the incremental strains using in the U.L. formulation

$${}^t\bar{e}_{1i} = \sum_{\substack{j=2 \\ j \neq 7}}^N {}^t\bar{\mathbf{B}}_{Lij} {}^t\bar{u}^j + ({}^t\bar{e}_{11} - {}^{t-\Delta t}\bar{e}_{11})\delta_{1i} \quad (32)$$

where the ${}^t\bar{\mathbf{B}}_{Lij}$ are the components of the linear strain–displacement matrix given in Table III(B) and δ_{ij} is the Kronecker delta; also

$${}^t\bar{e}_{11} = ({}^t\mathbf{L} - {}^0\mathbf{L})/{}^0\mathbf{L}$$

Using the T.L. formulation the corresponding calculations are

$${}^0\bar{e}_{1i} = \sum_{j=1}^{12} {}^0\bar{\mathbf{B}}_{Lij} {}^0\bar{u}^j + ({}^0\bar{e}_{11} - {}^{t-\Delta t}\bar{e}_{11})\delta_{1i} \quad (33)$$

where the constraints

$${}^0\bar{u}^1 = ({}^t\bar{\mathbf{R}}_{12} {}^0\bar{u}^2 + {}^t\bar{\mathbf{R}}_{13} {}^0\bar{u}^3)/{}^t\bar{\mathbf{R}}_{11}; \quad {}^0\bar{u}^7 = ({}^t\bar{\mathbf{R}}_{12} {}^0\bar{u}^8 + {}^t\bar{\mathbf{R}}_{13} {}^0\bar{u}^9)/{}^t\bar{\mathbf{R}}_{11} \quad (34)$$

should be imposed to evaluate the appropriate normal strains.

With the incremental strains known, the corresponding stress increments can be calculated as usual.¹⁵ In general large displacement and elastic–plastic analysis, the stiffness matrices and nodal point force vectors must be evaluated using numerical integration. Also, to improve the solution accuracy it may be necessary to employ equilibrium iterations in the incremental solution. The iterative equations are directly obtained from equations (14) and (15) in the usual manner.¹²

COMPARISON OF T.L. AND U.L. FORMULATIONS

In the T.L. formulation the reference co-ordinate system used is given by the element principal axes of inertia in the configuration at time 0, ${}^0\bar{x}_i$ ($i = 1, 2, 3$). Therefore, the complete stiffness matrix (including the linear and nonlinear strain stiffness matrices), the nodal point force vector and the local displacement increments are referred to this co-ordinate system and must be transformed to the global co-ordinate system 0x_i ($i = 1, 2, 3$):

$$\begin{aligned} {}^0\mathbf{K} &= {}^0\mathbf{R}^T {}^t\bar{\mathbf{K}} {}^0\mathbf{R} \\ {}^0\mathbf{F} &= {}^0\mathbf{R}^T {}^t\bar{\mathbf{F}} \\ \mathbf{u} &= {}^0\mathbf{R}^T {}^0\bar{\mathbf{u}} \end{aligned} \quad (35)$$

where ${}^0\mathbf{R}$ is the transformation matrix that expresses the nodal point displacements measured in the beam local co-ordinate system ${}^0\bar{x}_i$ ($i = 1, 2, 3$) in terms of the global nodal point displacements.

The reference co-ordinate system used in the U.L. formulation is defined by the principal axes of the beam element in the position at time t , i.e. ${}^t\bar{x}_i$ ($i = 1, 2, 3$). Therefore, the local stiffness matrix and the nodal point force vector are referred to this co-ordinate system. These

matrices are transformed to the global co-ordinate system using

$$\begin{aligned} {}^t\mathbf{K} &= {}^t\mathbf{R}^T {}^t\bar{\mathbf{K}} {}^t\mathbf{R} \\ {}^t\mathbf{F} &= {}^t\mathbf{R}^T {}^t\bar{\mathbf{F}} \\ \mathbf{u} &= {}^t\mathbf{R}^T \bar{\mathbf{u}} \\ {}^t\mathbf{R} &= {}^t\bar{\mathbf{R}} {}^0\mathbf{R} \end{aligned} \quad (36)$$

where ${}^t\bar{\mathbf{R}}$ is the transformation matrix relating the co-ordinate systems ${}^t\bar{x}_i$ and ${}^0\bar{x}_i$ ($i = 1, 2, 3$), as defined in equation (22).

The principal difference between the U.L. and the T.L. formulations is that in the T.L. formulation the transformation on the interpolation functions in equation (18) is carried out to refer the displacement interpolations to the original configuration, and the ${}^0\bar{\mathbf{B}}_{L1}$ matrix is included in the calculations. The transformations on the interpolation functions and the use of the ${}^0\bar{\mathbf{B}}_{L1}$ matrix in the T.L. formulation together are equivalent to the additional transformation matrix ${}^t\bar{\mathbf{R}}$ that is employed in equation (36) in the U.L. formulation. Indeed, as shown in more detail in the Appendix, using these formulations the same element stiffness matrices and nodal point force vectors are obtained.

Although the same final element stiffness matrices and nodal point force vectors are generated in the two formulations, it is noted that using numerical integration the transformation on the interpolation functions in equation (18) and the evaluation of the ${}^0\bar{\mathbf{B}}_{L1}$ matrix is carried out at each integration point. Therefore, the U.L. formulation is computationally more effective.

SAMPLE SOLUTIONS

The updated Lagrangian-based beam element was implemented in the computer program ADINA¹⁷ and a number of sample analyses were carried out. We report here the results of some of the analyses. In these analyses the beam linear strain stiffness matrices ${}^t\bar{\mathbf{K}}_L$ were evaluated in closed form, and the nonlinear strain stiffness matrices ${}^t\bar{\mathbf{K}}_{NL}$ and force vectors ${}^t\bar{\mathbf{F}}$ (see Table I) were evaluated using Newton–Cotes integration¹⁶. Also, in all analyses beam shear deformations were neglected.

Large deflection analysis of a shallow arch

The clamped circular arch with a single static load at the apex was analysed for buckling using the beam element, as shown in Figure 5. The material of the arch was assumed to be isotropic linear elastic. One half of the arch was idealized using 6, 12 and 18 equal beam elements. The same arch was also analysed using eight six-node isoparametric elements with 2×2 Gauss integration.

This arch was also analysed by Mallet and Berke, who used four ‘equilibrium-based’ elements.¹⁰ Dupuis *et al.*¹¹ analysed the same arch using curved beam elements, and used this example to demonstrate the convergence of their ‘Lagrangian’ and ‘updated’ formulations.

Figure 5 shows the predicted load–deflection curve of the arch. It is observed that in this analysis the use of the beam elements is quite effective.

Large deflection and rotation analyses of a cantilever beam

The objective in this analysis was to investigate the performance of the beam element in large displacement and rotation problems. Two problems were analysed. First, a large deflection and

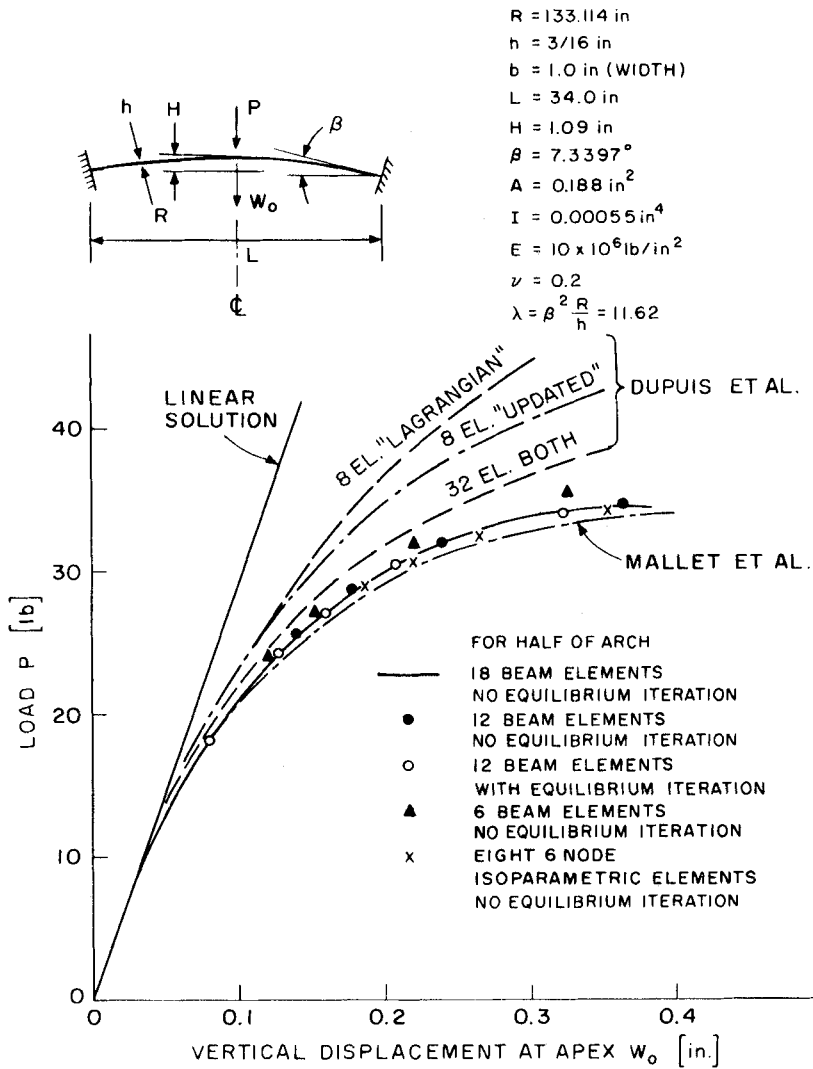
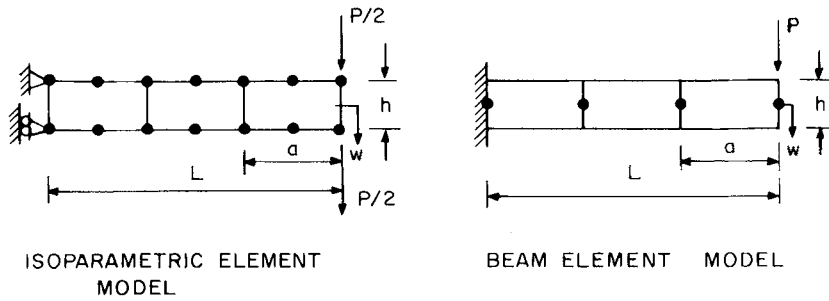


Figure 5. Large deflection analysis of shallow arch under concentrated load.

moderate rotation analysis of a clamped cantilever with a concentrated end load was carried out as shown in Figure 6. The second problem was the large displacement and large rotation analysis of a cantilever beam subjected to a concentrated end moment (Figure 7).

In the cantilever analysis subjected to the concentrated tip load, the objective was to demonstrate the effects of the aspect ratio of an element on its performance in the geometric nonlinear range. Figure 6 shows the response predicted by ADINA using four different models and an analytical solution.⁹ It is noted that the cantilever models using beam elements and two-dimensional isoparametric elements (2×2 Gauss integration), with an aspect ratio of 2, predict responses quite close to the analytical solution, and that the performance of the



- BEAM ELEMENTS, $\frac{a}{h} = 4$ & $\frac{a}{h} = 40$
- - - - ISOPARAMETRIC ELEMENTS, $\frac{a}{h} = 2$
- - - - ISOPARAMETRIC ELEMENTS, $\frac{a}{h} = 100$

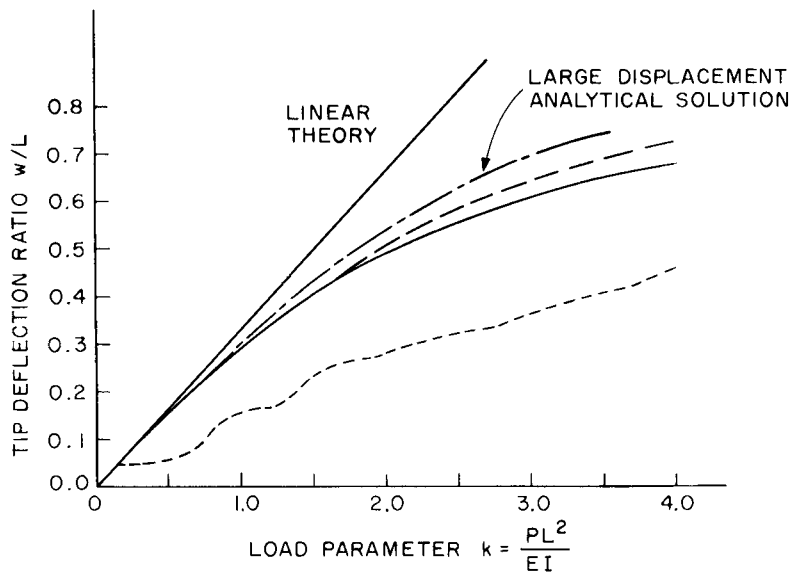


Figure 6. Large deflection analysis of a cantilever subjected to a concentrated load.

beam element does not change with its aspect ratio. However, as is well known, the predicted response using two-dimensional isoparametric elements deviates from the analytical solution with increasing element aspect ratios.

Figure 7 shows the results obtained in the analysis of the cantilever subjected to an end moment. The cantilever was modelled using 5 and 20 beam elements. The figure shows that the predicted response compares well with the analytical solution up to 90 degrees rotation.¹⁸ It is also seen that as the number of elements increases the numerically predicted response improves. This increase in accuracy is due to the fact that the geometry of the deformed cantilever is defined more accurately with a larger number of elements.

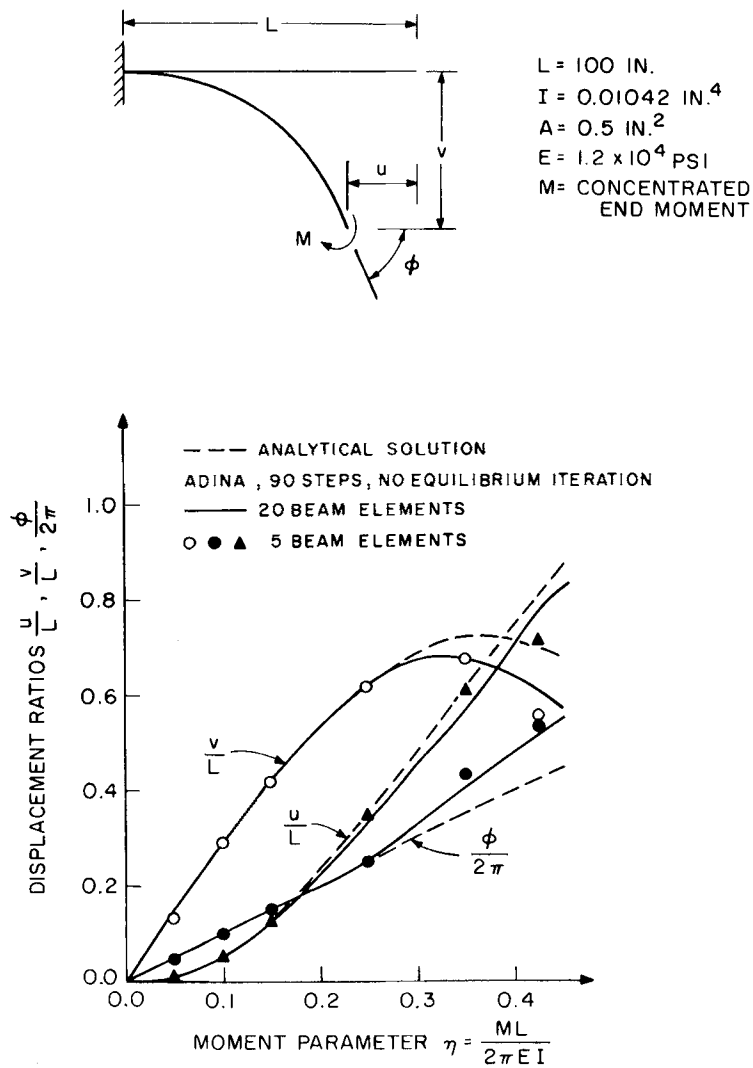


Figure 7. Moment-deflection curve.

Large displacement three-dimensional analysis of a 45-degree bend

The large displacement response of a cantilever 45-degree bend subjected to a concentrated end load, as shown in Figure 8, was calculated. The bend has an average radius of 100 in, cross-sectional area 1 in² and lies in the X-Y plane. The concentrated tip load is applied into the Z-direction.

The bend was idealized using 8 equal straight beam elements and 16 sixteen-node three-dimensional solid elements. For the beam elements the Newton-Cotes formula of order 3 × 3 × 3 was used and, for the isoparametric elements, Gauss integration of order 2 × 2 × 2 was employed.¹⁶ The material was assumed to be linear elastic.

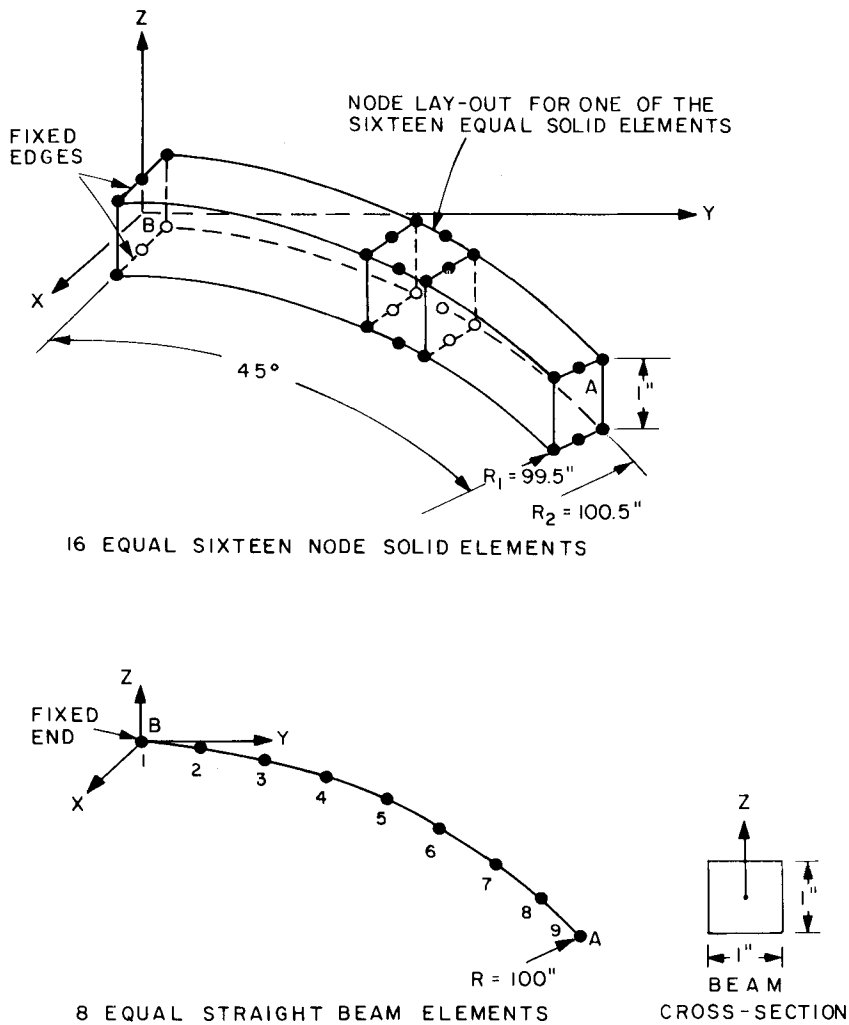


Figure 8. Finite element modelling of a 45-degree circular bend.

Figure 9 shows the tip deflection predicted by ADINA using the two finite element models. To the accuracy that can be shown in the illustration, the same response is predicted using the beam element idealization and the isoparametric element discretization. The deflected shapes of the bend at various load levels are shown in Figure 10.

CONCLUSIONS

To develop capabilities for large displacement and large rotation analysis of beam structures, an updated Lagrangian and a total Lagrangian formulation of a geometric nonlinear beam element

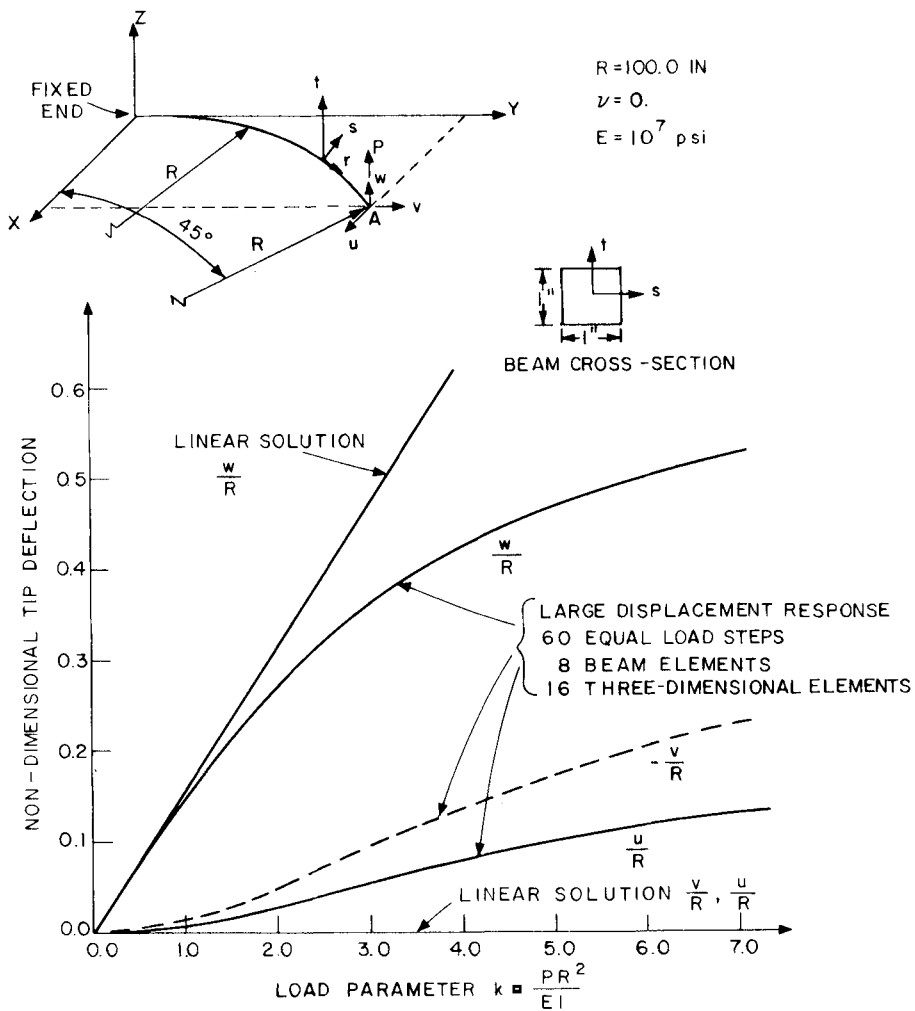


Figure 9. Three-dimensional large deflection analysis of a 45-degree circular bend.

have been presented. The incremental displacement fields within the straight two-noded beam element are defined using the usual beam displacement functions. It has been shown that the two formulations yield identical element stiffness matrices and nodal point force vectors, and that the updated Lagrangian formulation is computationally more effective. This formulation can be used efficiently for the general nonlinear analysis of beam structures.

ACKNOWLEDGEMENT

The work reported in this paper has been supported financially by the ADINA users group. We would like to acknowledge gratefully this support.

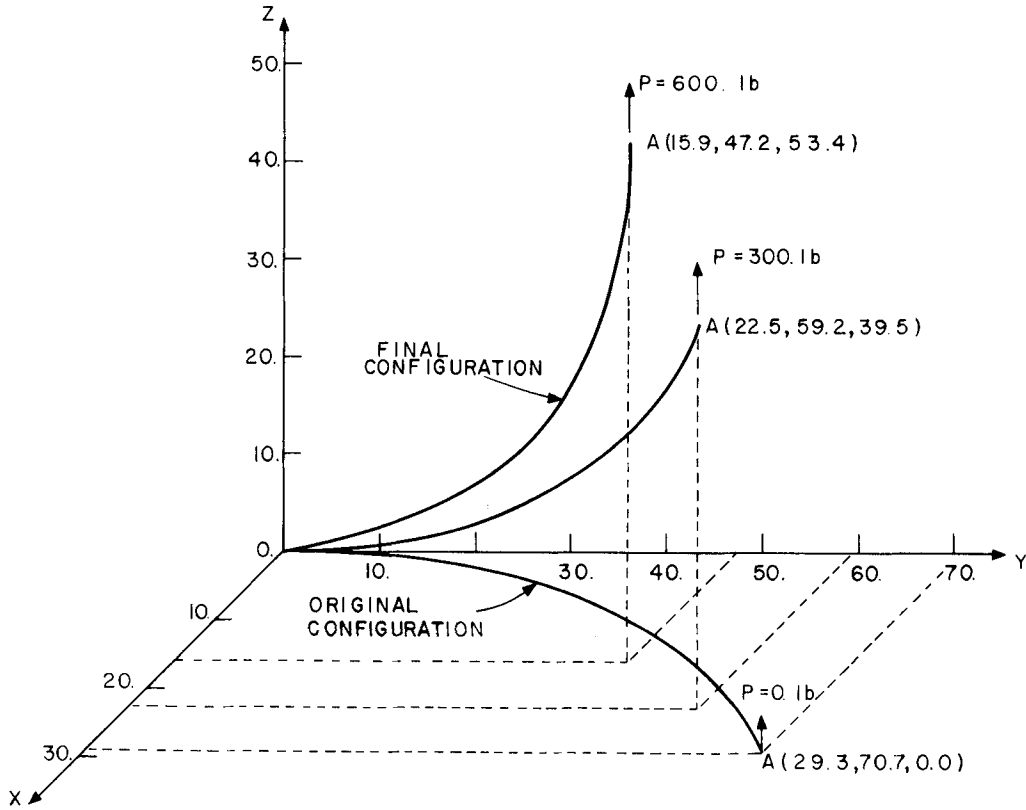


Figure 10. Deformed configurations of a 45-degree circular bend.

APPENDIX: DETAILED COMPARISON OF BEAM T.L. AND U.L. FORMULATIONS

In the text we showed that the U.L. formulation is more effective than the T.L. formulation for beam analysis. The objective in this appendix is to compare the T.L. and U.L. formulations presented in detail. Assume that the beam is deformed to the configuration at time t , as shown in Figure 3. It is shown in this appendix that all element matrices are identical in both formulations.

Linear strain stiffness matrices

Consider first the *T.L. formulation*. The initial displacement effect is taken into account using equation (20). Thus we have corresponding to Table III(A)

$$l_{ij} = {}^t\bar{R}_{ij} - \delta_{ij} \quad \begin{matrix} (i = 1, 2, 3) \\ (j = 1, 2, 3) \end{matrix} \quad (37)$$

The ${}^t\bar{R}_{ij}$ are the direction cosines of the ${}^t\bar{x}_i$ axes with respect to the ${}^0\bar{x}_i$ axes defined in equation (23), and δ_{ij} is the Kronecker delta. Using equation (37) the ${}^0\bar{\mathbf{B}}_{L1}$ matrix defined in Table III(A) is

$${}^0\bar{\mathbf{B}}_{L1} = \begin{bmatrix} ({}^t\bar{R}_{11} - 1) {}_0\mathbf{h}_{,1}^1 + {}^t\bar{R}_{21} {}_0\mathbf{h}_{,1}^2 + {}^t\bar{R}_{31} {}_0\mathbf{h}_{,1}^3 \\ ({}^t\bar{R}_{11} - 1) {}_0\mathbf{h}_{,2}^1 + {}^t\bar{R}_{12} {}_0\mathbf{h}_{,1}^1 + {}^t\bar{R}_{21} {}_0\mathbf{h}_{,2}^2 + ({}^t\bar{R}_{22} - 1) {}_0\mathbf{h}_{,1}^2 + {}^t\bar{R}_{31} {}_0\mathbf{h}_{,2}^3 + {}^t\bar{R}_{32} {}_0\mathbf{h}_{,1}^3 \\ ({}^t\bar{R}_{11} - 1) {}_0\mathbf{h}_{,3}^1 + {}^t\bar{R}_{13} {}_0\mathbf{h}_{,1}^1 + {}^t\bar{R}_{21} {}_0\mathbf{h}_{,3}^2 + {}^t\bar{R}_{23} {}_0\mathbf{h}_{,1}^2 + {}^t\bar{R}_{31} {}_0\mathbf{h}_{,3}^3 + ({}^t\bar{R}_{33} - 1) {}_0\mathbf{h}_{,1}^3 \end{bmatrix} \quad (38)$$

where (not considering shear deformations)

$${}^0\mathbf{h}^i = [{}^0h_{1,i}^i \ {}^0h_{2,i}^i \ \dots \ {}^0h_{12,i}^i] \quad (39)$$

Adding the ${}^i\bar{\mathbf{B}}_{L1}$ matrix of equation (38) to the matrix ${}^i\bar{\mathbf{B}}_{L0}$ defined in Table III(A) yields the linear strain-displacement matrix,

$${}^i\bar{\mathbf{B}}_L = \begin{bmatrix} {}^i\bar{\mathbf{R}}_{11} & {}^i\bar{\mathbf{R}}_{21} & {}^i\bar{\mathbf{R}}_{31} & 0 & 0 & 0 & 0 & 0 & 0 \\ {}^i\bar{\mathbf{R}}_{12} & {}^i\bar{\mathbf{R}}_{22} & {}^i\bar{\mathbf{R}}_{32} & {}^i\bar{\mathbf{R}}_{11} & {}^i\bar{\mathbf{R}}_{21} & {}^i\bar{\mathbf{R}}_{31} & 0 & 0 & 0 \\ {}^i\bar{\mathbf{R}}_{13} & {}^i\bar{\mathbf{R}}_{23} & {}^i\bar{\mathbf{R}}_{33} & 0 & 0 & 0 & {}^i\bar{\mathbf{R}}_{11} & {}^i\bar{\mathbf{R}}_{21} & {}^i\bar{\mathbf{R}}_{31} \end{bmatrix} \begin{bmatrix} {}^0\mathbf{H}_{,1} \\ {}^0\mathbf{H}_{,2} \\ {}^0\mathbf{H}_{,3} \end{bmatrix} \quad (40)$$

where we define

$${}_\tau\mathbf{H}_{,i} = \begin{bmatrix} {}_\tau\mathbf{h}_{,i}^1 \\ {}_\tau\mathbf{h}_{,i}^2 \\ {}_\tau\mathbf{h}_{,i}^3 \end{bmatrix} \quad (\tau = 0, t) \quad (41)$$

The derivatives of the interpolation functions ${}^0h_k^i$ defined in equation (18) are

$${}^0h_{k,j}^i = \sum_{m=1}^3 \sum_{n=1}^{12} {}^i\bar{\mathbf{R}}_{im} {}^t\mathbf{h}_{n,j}^m {}^i\bar{\mathbf{R}}_{nk} \quad \begin{matrix} (i = 1, 2, 3) \\ (j = 1, 2, 3) \end{matrix} \quad (42)$$

where the incremental interpolation functions ${}^t\mathbf{h}^{m,n}$ are defined in Table III. Equations (42) may be rewritten in matrix form

$$\begin{bmatrix} {}^0\mathbf{H}_{,1} \\ {}^0\mathbf{H}_{,2} \\ {}^0\mathbf{H}_{,3} \end{bmatrix} = \begin{bmatrix} {}^i\bar{\mathbf{R}} & \mathbf{0} & \mathbf{0} \\ \mathbf{0} & {}^i\bar{\mathbf{R}} & \mathbf{0} \\ \mathbf{0} & \mathbf{0} & {}^i\bar{\mathbf{R}} \end{bmatrix} \begin{bmatrix} {}^t\mathbf{H}_{,1} \\ {}^t\mathbf{H}_{,2} \\ {}^t\mathbf{H}_{,3} \end{bmatrix} {}^i\bar{\mathbf{R}} \quad (43)$$

where ${}^i\bar{\mathbf{R}}$ and ${}^t\bar{\mathbf{R}}$ are defined in equations (22) and (23), respectively. Substituting equations (43) into equation (40) and simplifying gives,

$${}^i\bar{\mathbf{B}}_L = \begin{bmatrix} {}^t\mathbf{h}_{,1}^1 \\ ({}^t\mathbf{h}_{,1}^2 + {}^t\mathbf{h}_{,2}^1) \\ ({}^t\mathbf{h}_{,1}^3 + {}^t\mathbf{h}_{,3}^1) \end{bmatrix} {}^i\bar{\mathbf{R}} \quad (44)$$

In the *U.L. formulation* the geometric linear strain-displacement matrix is given in Table III(B)

$${}^i\bar{\mathbf{B}}_L = \begin{bmatrix} {}^t\mathbf{h}_{,1}^1 \\ ({}^t\mathbf{h}_{,1}^2 + {}^t\mathbf{h}_{,2}^1) \\ ({}^t\mathbf{h}_{,1}^3 + {}^t\mathbf{h}_{,3}^1) \end{bmatrix} \quad (45)$$

Comparing equations (44) and (45) yields

$${}^i\bar{\mathbf{B}}_L = {}^i\bar{\mathbf{B}}_L {}^i\bar{\mathbf{R}} \quad (46)$$

Substituting the above relation into Table I to evaluate the linear strain stiffness matrices in both formulations, and comparing, we obtain

$${}^i\bar{\mathbf{K}}_L = {}^i\bar{\mathbf{R}}^T {}^i\bar{\mathbf{K}}_L {}^i\bar{\mathbf{R}} \quad (47)$$

Therefore the two formulations lead to identical linear-strain stiffness matrices corresponding to the global co-ordinate system.

Nodal point force vectors

The components of the Cauchy stress tensor referred to the ${}^t\bar{x}_i$ axes are numerically equal to the components of the 2nd Piola–Kirchhoff stress tensor referred to the ${}^0\bar{x}_i$ axes, i.e. the stress vectors ${}^t\bar{\tau}$ and ${}^0\bar{\hat{S}}$ [as defined in Table III] are equal. It follows from equation (46), Table I and the above fact that the nodal point force vectors corresponding to the global axes are equal in both formulations.

Nonlinear strain stiffness matrices

The nonlinear strain–displacement matrix in the *T.L. formulation* is defined in Table III(A):

$${}^0\bar{\mathbf{B}}_{NL} = \begin{bmatrix} {}_0\mathbf{H}_{,1} \\ {}_0\mathbf{H}_{,2} \\ {}_0\mathbf{H}_{,3} \end{bmatrix} \tag{48}$$

Substituting equation (43) into (48) gives

$${}^0\bar{\mathbf{B}}_{NL} = \begin{bmatrix} {}^t\bar{\mathbf{R}} & \mathbf{0} & \mathbf{0} \\ \mathbf{0} & {}^t\bar{\mathbf{R}} & \mathbf{0} \\ \mathbf{0} & \mathbf{0} & {}^t\bar{\mathbf{R}} \end{bmatrix} \begin{bmatrix} {}^t\mathbf{H}_{,1} \\ {}^t\mathbf{H}_{,2} \\ {}^t\mathbf{H}_{,3} \end{bmatrix} {}^t\bar{\mathbf{R}} \tag{49}$$

The geometric nonlinear stiffness matrix is evaluated as defined in Table I,

$${}^0\bar{\mathbf{K}}_{NL} = {}^t\bar{\mathbf{R}}^T \left\{ \int_V \begin{bmatrix} {}^t\mathbf{H}_{,1} \\ {}^t\mathbf{H}_{,2} \\ {}^t\mathbf{H}_{,3} \end{bmatrix}^T \begin{bmatrix} {}^t\bar{\mathbf{R}} & \mathbf{0} & \mathbf{0} \\ \mathbf{0} & {}^t\bar{\mathbf{R}} & \mathbf{0} \\ \mathbf{0} & \mathbf{0} & {}^t\bar{\mathbf{R}} \end{bmatrix}^T {}^0\bar{\mathbf{S}} \right. \tag{50}$$

$$\left. \begin{bmatrix} {}^t\bar{\mathbf{R}} & \mathbf{0} & \mathbf{0} \\ \mathbf{0} & {}^t\bar{\mathbf{R}} & \mathbf{0} \\ \mathbf{0} & \mathbf{0} & {}^t\bar{\mathbf{R}} \end{bmatrix} \begin{bmatrix} {}^t\mathbf{H}_{,1} \\ {}^t\mathbf{H}_{,2} \\ {}^t\mathbf{H}_{,3} \end{bmatrix} dv \right\} {}^t\bar{\mathbf{R}}$$

where the 2nd Piola–Kirchhoff stress matrix is given in Table III(A). We also have

$$\begin{bmatrix} {}^t\bar{\mathbf{R}} & \mathbf{0} & \mathbf{0} \\ \mathbf{0} & {}^t\bar{\mathbf{R}} & \mathbf{0} \\ \mathbf{0} & \mathbf{0} & {}^t\bar{\mathbf{R}} \end{bmatrix}^T {}^0\bar{\mathbf{S}} \begin{bmatrix} {}^t\bar{\mathbf{R}} & \mathbf{0} & \mathbf{0} \\ \mathbf{0} & {}^t\bar{\mathbf{R}} & \mathbf{0} \\ \mathbf{0} & \mathbf{0} & {}^t\bar{\mathbf{R}} \end{bmatrix} = {}^0\bar{\mathbf{S}} \tag{51}$$

and the ${}^t\mathbf{h}_{,2}^2$ and ${}^t\mathbf{h}_{,3}^3$ are null vectors. Thus equation (50) can be written as

$${}^0\bar{\mathbf{K}}_{NL} = {}^t\bar{\mathbf{R}}^T \left\{ \int_V {}^t\bar{\mathbf{B}}_{NL}^T {}^0\bar{\mathbf{S}} {}^t\bar{\mathbf{B}}_{NL} dv \right\} {}^t\bar{\mathbf{R}} \tag{52}$$

where the matrix ${}^t\bar{\mathbf{B}}_{NL}$ is defined in Table III(B), and

$${}^0\bar{\mathbf{S}} = \begin{bmatrix} {}^0\bar{\mathbf{S}}_{11} & & & & & & & \\ 0 & {}^0\bar{\mathbf{S}}_{11} & & & & & & \\ 0 & 0 & {}^0\bar{\mathbf{S}}_{11} & & & & & \\ {}^0\bar{\mathbf{S}}_{12} & 0 & 0 & 0 & & & & \\ 0 & 0 & {}^0\bar{\mathbf{S}}_{12} & 0 & 0 & & & \\ {}^0\bar{\mathbf{S}}_{13} & 0 & 0 & 0 & 0 & 0 & & \\ 0 & {}^0\bar{\mathbf{S}}_{13} & 0 & 0 & 0 & 0 & 0 & 0 \end{bmatrix} \tag{53}$$

Symmetric

The geometric nonlinear stiffness matrix based on the *U.L. formulation* is evaluated by using the matrices of Table III,

$${}^i\bar{\mathbf{K}}_{NL} = \int_V {}^i\bar{\mathbf{B}}_{NL}^T {}^i\bar{\boldsymbol{\tau}} {}^i\bar{\mathbf{B}}_{NL} dv \quad (54)$$

Since the stress vectors ${}^i\hat{\boldsymbol{\tau}}$ and ${}^i_0\hat{\mathbf{S}}$ are numerically identical for the beam element we have

$${}^i_0\bar{\mathbf{K}}_{NL} = {}^i\bar{\mathbf{R}}^T {}^i\bar{\mathbf{K}}_{NL} {}^i\bar{\mathbf{R}} \quad (55)$$

Therefore the two formulations lead to identical nonlinear strain stiffness matrices corresponding to the global co-ordinate system.

REFERENCES

1. J. H. Argyris and P. C. Dunne, 'A simple theory of geometrical stiffness with application to beam and shell problems', *2nd Int. Symp. Computing Meth. Appl. Sci. & Engng*, Versailles, France (1975); *ISD-Report No. 183*, Univ. of Stuttgart (1975).
2. Z. P. Bazant and M. E. Nimeiri, 'Large-deflection spatial buckling of thin-walled beams and frames', *ASCE, J. Eng. Mech. Div.*, 10247-10281 (1973).
3. C. Oran and A. Kassimaili, 'Large deflection of framed structures under static and dynamic loads', *Comp. & Struct.* **6**, 536-547 (1976).
4. R. W. H. Wu and E. A. Witmer, 'Nonlinear transient responses of structures by the spatial finite element method,' *AIAA J.* **11**(8), 1110-1117 (1973).
5. T. Y. Yang, 'Matrix displacement solution to elastica problems of beams and frames', *Int. J. Sol. Struct.* **9**, 828-842 (1973).
6. C. Orean, 'Tangent stiffness in plane frames', *J. Struct. Div., ASCE*, **99** (ST6), 973-985 (1973).
7. T. Belytschko, L. Schwer and M. J. Klein, 'Large displacement transient analysis of space frames', *Int. J. Num. meth. Engng*, **11**, 65-84 (1977).
8. S. Ranganath and R. J. Clifton, 'Finite deflection dynamics of elastic beams', *Int. J. Sol. Struct.* **10**, 557-568 (1974).
9. J. T. Holden, 'On the finite deflections of thin beams', *Int. J. Sol. Struct.* **8**, 1051-1055 (1972).
10. R. H. Mallet and L. Berke, 'Automated method for the large deflection and instability analysis of three-dimensional truss and frame assemblies', *AFFDL-TR-66-102*, (1966).
11. G. A. Dupuis, H. D. Hibbitt, S. F. McNamara and P. V. Marcal, 'Nonlinear material and geometric behavior of shell structures', *Comp. & Struct.* **1**, 223-239 (1971).
12. K. J. Bathe, E. Ramm and E. L. Wilson, 'Finite element formulations for large deformation dynamic analysis', *Int. J. num. Meth. Engng*, **9**, 353-386 (1975).
13. K. J. Bathe, 'An assessment of current finite element analysis of nonlinear problems in solid mechanics', *Symp. Num. Solutions of Partial Diff. Eqns*, Univ. Maryland (1975).
14. K. J. Bathe, 'Finite element formulation, modeling and solution of nonlinear dynamic problems', in *Numerical Methods for Partial Differential Equations* (Ed. S. V. Parter), Academic Press, 1979.
15. K. J. Bathe, 'Static and dynamic geometric and material nonlinear analysis using ADINA', *Report 82448-2*, Acoustics and Vibration Lab., Mechanical Engineering Dept., MIT (1977).
16. K. J. Bathe and E. L. Wilson, *Numerical Methods in Finite Element Analysis*, Prentice-Hall, Englewood Cliffs, N.J., 1976.
17. K. J. Bathe, 'ADINA - A finite element program for automatic dynamic incremental nonlinear analysis', *Report 82448-1*, Acoustics and Vibration Lab., Mechanical Engineering Dept., MIT (1977).
18. E. Ramm, 'A plate/shell element for large deflections and rotations', in *Formulations and Computational Algorithms in Finite Element Analysis*, (Eds. K. J. Bathe, J. T. Oden and W. Wunderlich), MIT Press, 1977.